LA-2000
PHYSICS AND MATHEMATICS
(TID-4500, 13th ed., Suppl.)

LOS ALAMOS SCIENTIFIC LABORATORY
OF THE UNIVERSITY OF CALIFORNIA LOS ALAMOS NEW MEXICO

REPORT WRITTEN: August 1947

REPORT DISTRIBUTED: March 27, 1958

BLAST WAVE*

by

Hans A. Bethe
Klaus Fuchs
Joseph O. Hirschfelder
John L. Magee
Rudolph E. Peierls
John von Neumann

*This report supersedes LA-1020 and part of LA-1021.

Contract W-7405-ENG. 36 with the U. S. Atomic Energy Commission

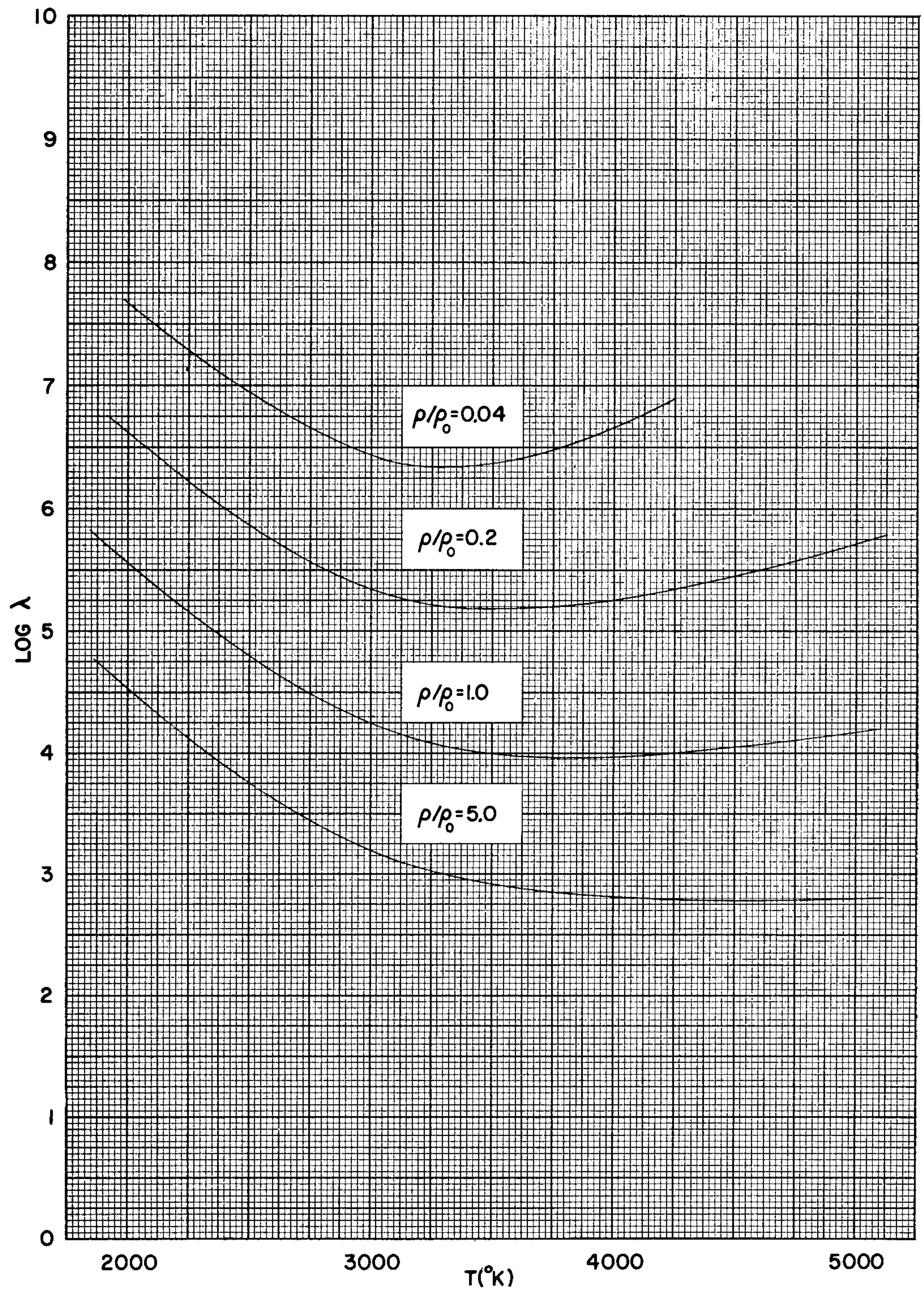

Fig. 3.6 Mean free path of radiation in NO_2; radiation the same temperature as the NO_2. $\lambda = 1/\bar{K}' \; P(NO_2)$

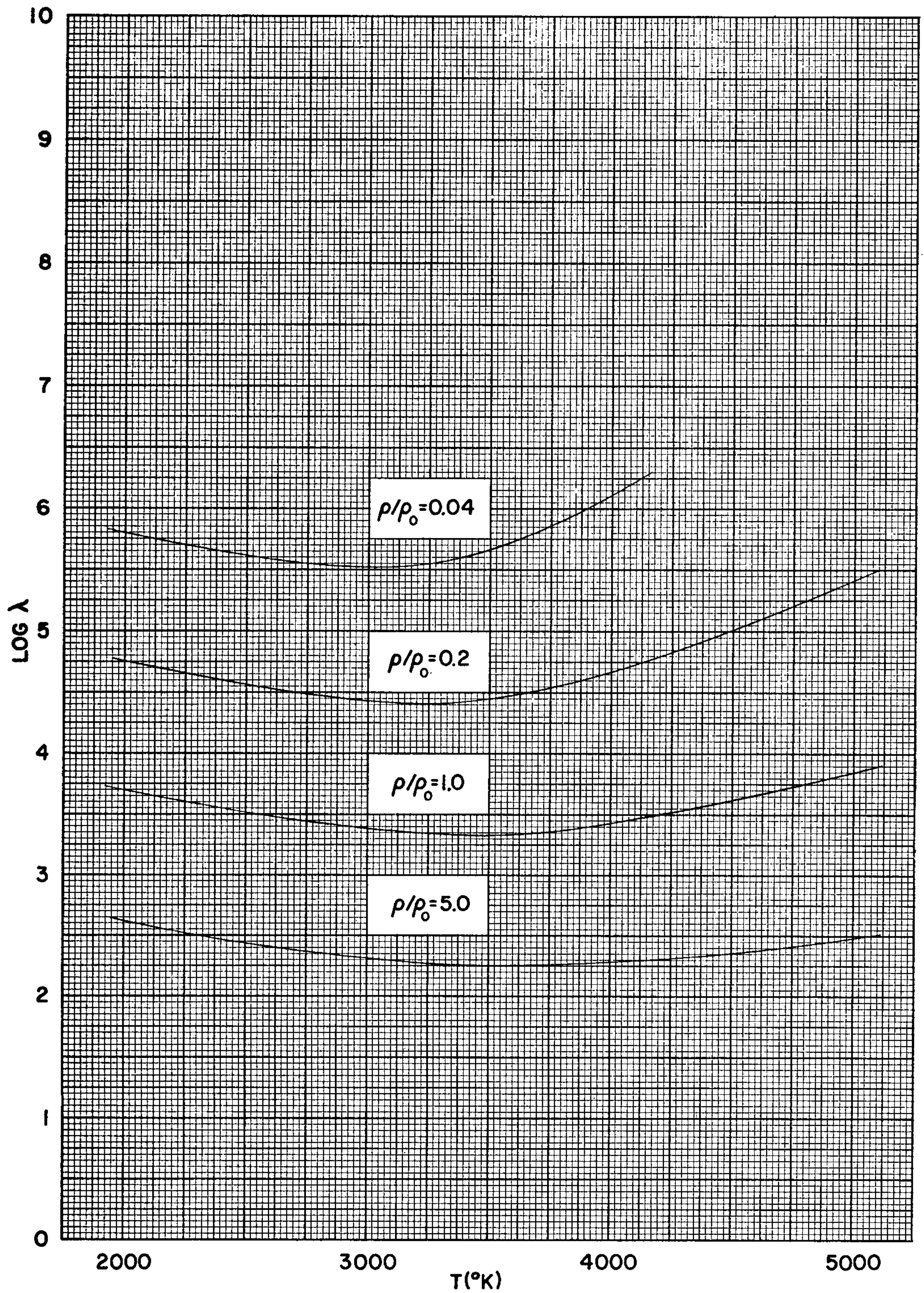

Fig. 3.7 Mean free path of radiation in NO_2; the radiation temperature above 10,000°K

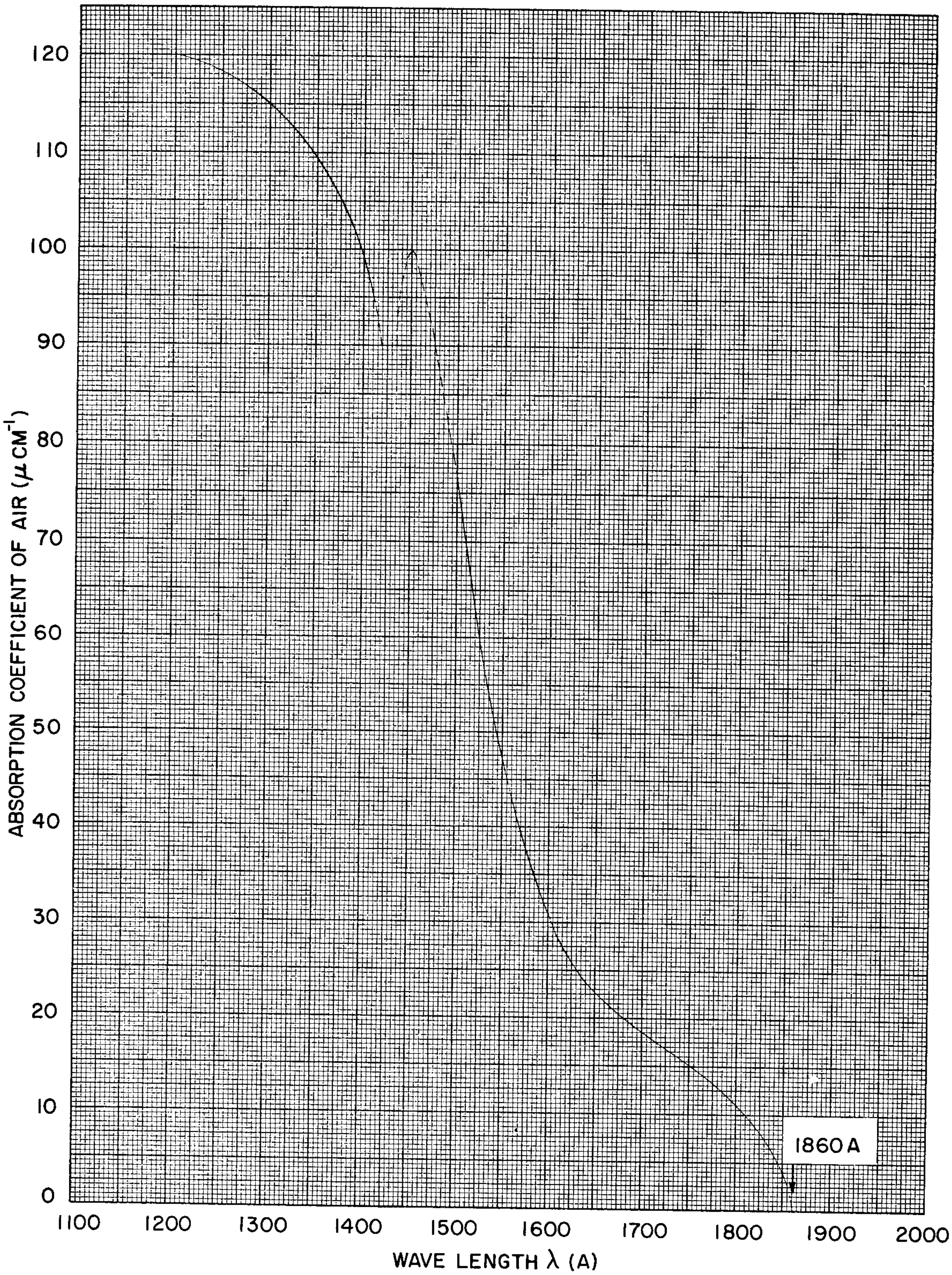

Fig. 3.8 Absorption of air; T = 300°K; p = 1 atm

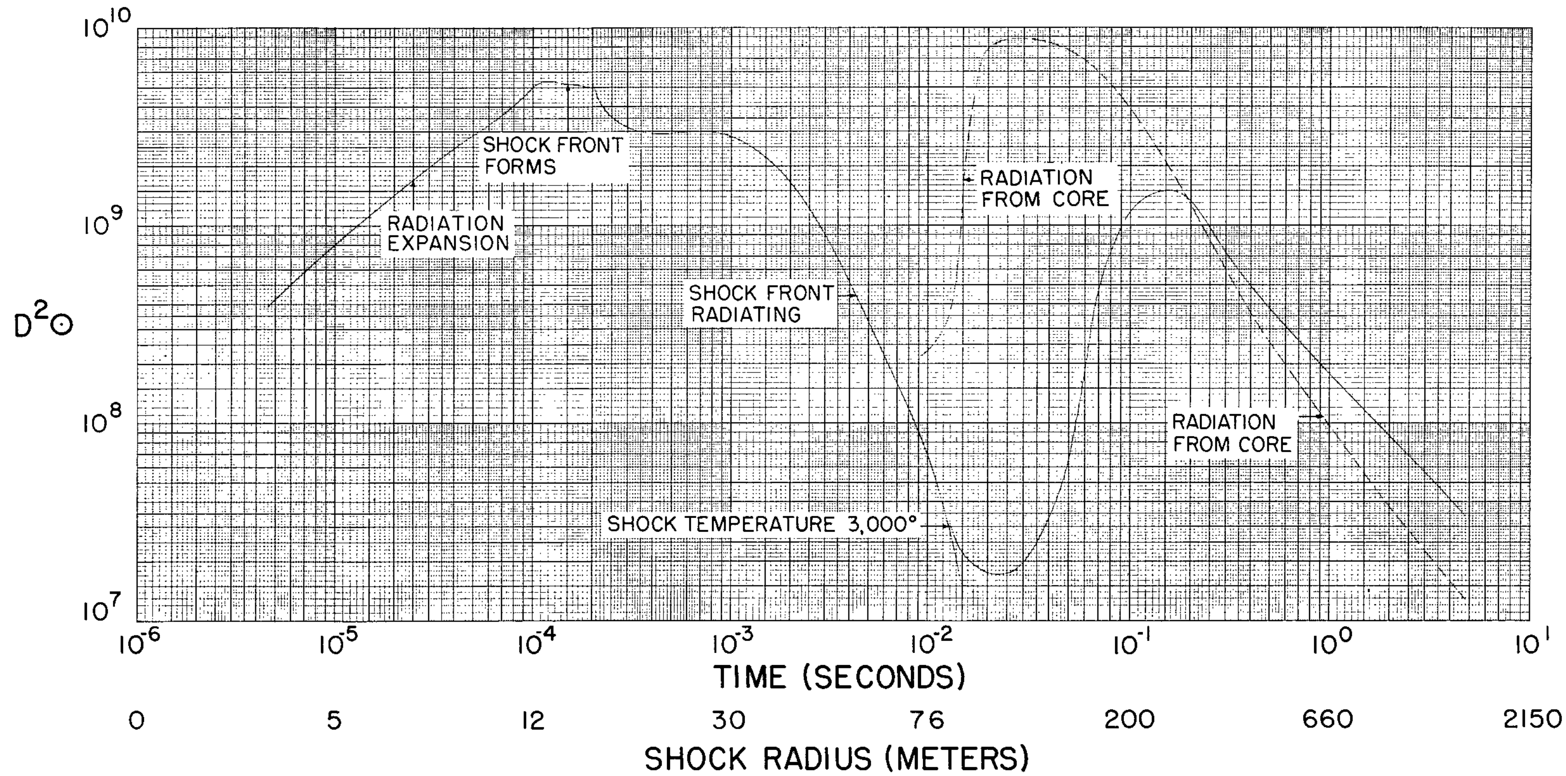

Fig. 3.10 Over-all time history of the blast wave

below 5000°K. Of course the air has no NO_2 at all before it enters the shock and so some time is required to form NO_2 after the air is heated by the shock. Formation of NO_2 in heated air under laboratory conditions has been studied by Daniels. Presumably the mechanism for formation is in two steps

(a) $N_2 + O_2 \rightarrow 2\ NO$

(b) $2\ NO + O_2 \rightarrow 2\ NO_2$

Reaction (b)[15] is extremely fast at all temperatures above 600°K and will always maintain equilibrium between NO, O_2 and NO_2. The rate of reaction (a) is strongly temperature dependent and so effectively one can say that it takes place above a certain temperature and does not occur below this temperature. We have selected 2000°K for this temperature from data furnished by Daniels.[16]

The NO_2 zone is therefore limited to the air which was initially within 100 meters, since the shock temperature is 2000°K at this distance.

<u>Last Stage of the Cooling.</u> At the time the core starts radiating most strongly, the shock front is most opaque and therefore the radiated energy

---

15. Hans J. Schumacker, <u>Chemische Gasreactionen,</u> T. Steinkopff, Dresden und Leipzig, 1938.

16. Farrington Daniels, private communication.

$$NO_2 + O_2 \underset{k_b}{\overset{k_j}{\rightleftarrows}} 2\ NO \qquad \begin{aligned} k_j &= 10^{8.5}\ \exp-(45{,}280/T)\ \ (\text{atm sec}^{-1}) \\ k_b &= 10^{9}\ \exp-(34{,}000/T)\ \ (\text{atm sec}^{-1}) \end{aligned}$$

Air at the shock front when the temperature is 2000°K has a pressure of about 10 atm O_2 and 40 atm N_2.

$$\frac{dp_{NO}}{dt} = 10^{8.5}\ e^{-22.640} \times 400 = 400 \times 10^{-1.33} = 18.7\ \text{atm/sec}$$

The rate of formation of NO is 0.019 atm/msec while the equilibrium partial pressure is 0.4 atm. The shock front moves about a meter per millisecond and so obviously the NO_2 equilibrium does not have time to be established. A similar calculation shows that at 2500°K the equilibrium is easily established within a millisecond. The indicated NO_2 "cutoff" is thus below 2500°K and we have arbitrarily taken 2000°K as the limit.

is essentially all absorbed behind the front. There are about two optical depths for high temperature radiation due to the NO_2 alone, and at this time O_2 in its lowest state is also very effective since the radiation has a temperature of about 40,000°K. We have not followed the decrease in opacity of the absorption layer as it expands, but by the time the shock front reaches 300 meters there is certainly negligible absorption of 20,000°K radiation by all outside layers. The ball of fire finally radiates as a hot mass of gas without self absorption. At the very last, only NO_2 can radiate visible light and so the ball of fire darkens as it drops to 2000°.

3.6 The Ball of Fire

The last two sections have described the effects of radiation in the formation and growth of the air blast. Except for the noted omissions,[17] this description is qualitatively complete for air blasts of this size. Other phenomena of interest have to do with the transmission of radiation energy ahead of the shock. Insofar as the description of the last two sections gives a complete model of the air blast, we can use it to determine the amount of energy transmitted through the shock front as a function of time. We also get a description of the quality (e.g., temperature) of the radiation, and the size and appearance of the ball of fire.

In the early phase, as long as the front is itself radiating strongly, there is a well-defined, spherical ball of fire. During this time the inner radiation front is, of course, not to be seen. When the shock front can no longer radiate, the hot core inside becomes more visible as the molecular absorbing layer becomes more tenuous. In the final stage, at the time of the second maximum and later, there is a hot core radiating, surrounded by a cooler fringe which is also radiating. At this time the ball has little absorption for its own radiation and is no longer a well-defined sphere with a sharp boundary.

The amount of radiant energy escaping per unit time into the air ahead of the shock front as a function of time is given in Fig. 3.10. This figure is largely schematic and has been obtained by methods which will be discussed below.

The unit $\odot$ (used in Fig. 3.10) is 1.35×10^6 ergs/cm^2/sec, the flux of radiant energy incident into the earth's outer atmosphere from the sun. D is measured in meters.

17. Effects of gamma radiation, bomb materials, turbulence.

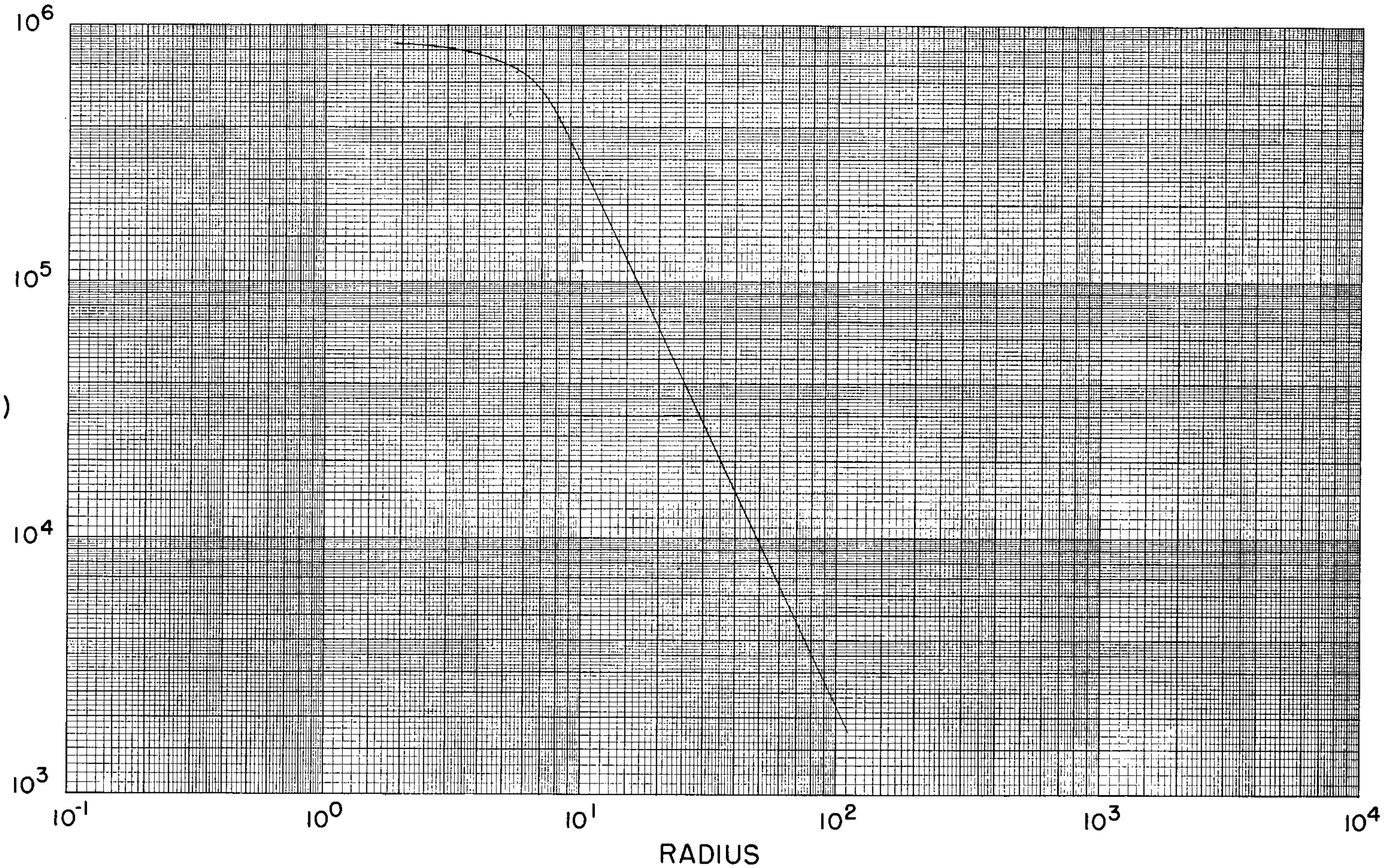

Fig. 3.11 Shock temperature vs shock radius

Chapter 6

THE IBM SOLUTION OF THE BLAST WAVE PROBLEM

by K. Fuchs

6.1 Introduction

The discussion in the preceding chapters shows that the problem of the propagation of the blast wave from a nuclear explosion is quite complicated. Even if we disregard any transport of radiation, appreciable complications arise in view of the large variations in temperature and entropy. We may roughly divide the range of shock temperatures into two regions. First, the region from about one million degrees to about three thousand degrees absolute; here dissociation of molecules and ionization of the atoms takes place; consequently $\gamma - 1$ is fairly small but varies with temperature. Second, below 3000°; here γ is less variable and approaches eventually the value 1.4 in normal conditions.

The temperature varies also, of course, along an adiabatic. However, the total variation between the shock pressure and 1 atm is not excessive – about a factor 2 at shock temperature of 3000°K and slightly more than a factor 10 for a shock temperature of 1,000,000°. The effect of decreasing temperature along the adiabatic on the degree of ionization or dissociation is partly balanced by the decrease in density. For this reason the variation of γ along an adiabatic is not as pronounced as one might expect from the change in temperature. Therefore qualitative statements made about the conditions at the shock front hold to a large degree also for the subsequent expansion behind the shock.

A temperature of 3000°K is reached in the shock when the shock pressure is about 80 atm. (For an energy release of 10,000 tons of TNT the shock radius is then 80 meters.) We are, however, more interested in the pressure region from about 1 atm down (corresponding to shock radii of 500 meters or more). It was felt that the exact energy distribution at this early stage could not have an appreciable effect on the pressure distribution in the later stages as long as the energy distribution is at least roughly correct. It was decided to start an IBM calculation at this point and to calculate the initial conditions for this instant by means of the approximations developed in the preceding chapters. The approximations made include (for details see Section 6.2):

(1) An approximate treatment of the isothermal sphere. In actual fact the isothermal sphere at this late stage has no significant influence on the propagation of the shock. However, in the first instance we are interested in the isothermal sphere as such; in the second instance the isothermal sphere greatly facilitates numerical computations, since it reduces the total range of temperatures and entropies which exist at any given moment, and eliminates the singularity at the centre.

(2) γ was assumed to be constant and an average value 1.25 was assumed. This is probably the least satisfactory of the assumptions made, but in view of the fact that we did not require a very accurate estimate of the initial conditions, and that a calculation with variable γ is hardly feasible without a great amount of computation, this assumption seemed justified.

(3) $\gamma - 1$ was assumed small. This assumption is not essential, but the error introduced thereby is small and it has the advantage that the isothermal sphere can be included as an integral part of the calculation.

For the IBM run it is of great advantage if the variation of the pressure along an adiabatic is a simple function of the density, though the variation from one adiabatic to another may be given in numerical form. In this case the adiabatic of each mass point is given by one or two constants and we require only a table of these constants as functions of one variable.

It would be difficult to find a simple presentation of the equation of state covering the whole region of adiabatics between the shock pressure curve and normal pressure. However, with the limitation to shock pressure below 80 atm the demand of a simple representation becomes feasible. In particular this is true for the adiabatics which start at shock pressures below 80 atm, since then no ionization or dissociation occurs. We require also, of course, the adiabatics of the inner mass points, which were shocked by stronger shocks. However we require only the tail end of these adiabatics. Furthermore, the highest entropies are eliminated by the equalization of entropy inside the isothermal sphere. The equation of state which has been used is discussed in Chapter 7. The requirement of a simple equation of state is the principal reason for starting the IBM run at such a comparatively late stage.

Although radiation transport has been taken into account insofar as it is responsible for the formation of the isothermal sphere, no allowance has been made for the radiation transport from the isothermal sphere into the region in which NO_2 is formed. As explained in Chapter 3, this transport of energy becomes important when the shock radius has reached about 100 meters and it should affect the propagation of the shock shortly thereafter. The opacity data required for the purpose of calculating this transport are not sufficiently well known.[1] In neglecting the radiation transport altogether we are pessimistic, since it is of advantage to have the energy close to the shock front. Then the shock pressure decreases less rapidly than it would otherwise. The increased shock pressure would naturally lead to a greater degree of dissipation of energy by the shock, so that at larger distances the shock pressure might drop again more rapidly, and at sufficiently large distances the effect of the radiation transport on the shock pressure would be reversed. At present we are not in a position to make any definite statement about this possibility.

The IBM run was intended for an energy release of 10,000 tons of TNT. Owing to some unfortunate circumstances related in Section 6.3, no definite energy can be attributed to the run throughout its whole history. At sufficiently large distances the energy should be assumed to be 13,000 tons. Other energies can, of course, be obtained by the usual scaling laws.

6.2 The Initial Conditions of the IBM Run

The initial conditions of the IBM run were prepared by Hirschfelder and Magee. The principal data are summarized below without going into the details of the calculation. All data are for an energy release of 10,000 tons of TNT.

6.2.1 The Isothermal Sphere[2]

The Lagrangian coordinate of the radiation front is given in terms of the shock radius by Eq. 3.64 of Chapter 3. It can be rewritten in the form

$$r_0 = \left[11.85\ Y^{0.7326} - 601.5\right]^{1/3}\ 100\ \text{cm} \tag{6.1}$$

Here both r_0 and Y are given in centimeters. It was convenient to choose

---

1. Chapter 3 contains a discussion of opacity data which postdates this statement.

2. Chapter 3 values are revised figures. Notations in equations used here are in the main those of Bethe in Chapter 4.

a simple value of Y/r_0 and the value 4 was chosen, which corresponds to a shock pressure very near to 80 atm. Then

$$r_0 = 1997 \text{ cm}, \; Y = 7987 \text{ cm}, \; Y/r_0 = 4 \tag{6.2}$$

The actual radius R_0 of the isothermal sphere is obtained from the conservation of mass. Since we assume constant density ρ and constant pressure in the isothermal sphere one has

$$\rho_0 r_0^3 = \rho R_0^3 \tag{6.3}$$

The value r_0 varies very slowly after the shock radius has reached about 10 meters, and the effect of the isothermal sphere on the shock is negligible a short while thereafter. Beyond a shock radius of 80 meters r_0 varies very slowly indeed.

It is a good assumption to assume that r_0 is constant. The actual radius R_0 then varies in accordance with Eq. 6.3 only because the air in the isothermal sphere expands. The initial value of R_0 is 60 meters.

The initial condition of the isothermal sphere is given by the following quantities:

Temperature = 49,000°K
Pressure = 37.0 atm
Density = 0.0392 × normal density
Entropy $\Delta s/R$ = 85
Internal energy and enthalpy $E/R = 1.487 \times 10^6$, $H/R = 1.782 \times 10^6$
R_0 = 60.23 meters
r_0 = 19.97 meters

These data were obtained from a calculation indicated below.

6.2.2 Initial Pressure and Density Distribution

It has been shown by Bethe in Chapter 4, Section 5, that the isothermal sphere can be treated on the assumption of small $\gamma - 1$. The small $\gamma - 1$ approximation has been checked for a point source solution (see Chapter 4, Sections 3 and 4) and it was found satisfactory in the region in which we are interested. Since the solution which we require is in any case very close to the point source solution except in the neighborhood of the isothermal sphere, the error of the small $(\gamma - 1)$ approximation is small.

We shall not go into the details of the calculation. The analysis is rather involved, but the lines along which it proceeds are sufficiently indicated in Bethe's Section 4.5. The resulting equations had previously been evaluated for two values of γ in order to see how sensitive they were to a change in γ. The values chosen were $\gamma = 1.2$ and $\gamma = 1.3$. The values for $\gamma = 1.25$ were then obtained by interpolation. In this way we find the initial pressure and density distribution as well as the velocities and the Eulerian coordinates of all mass points.

Some adjustments had to be made on the intial conditions. A minor adjustment arose from the fact that the small $\gamma - 1$ treatment of the isothermal sphere does not agree exactly with the treatment of Hirschfelder and Magee. The error, which may be due to either method, may be seen from the values of R_0/Y; the small $\gamma = 1$ treatment gives $R_0/Y = 0.850$ compared to 0.761 by means of the other method. The latter value was assumed to be more reliable.

Furthermore, at the start of the IBM calculation the value of γ at the shock front is larger than 1.25; instead of a compression ratio in the shock $\rho_s/\rho_0 = 9$, as would be expected for $\gamma = 1.25$, the value obtained from the correct Hugoniot curve for a pressure of 77.25 atm is $\rho_s/\rho_0 = 7.24$. The density contour was, therefore, adjusted to give the correct compression ratio at the shock, and the correct radius of the isothermal sphere. This required also an adjustment in the Eulerian coordinates R, since it is essential that the initial conditions satisfy the equation of continuity:

$$\frac{\rho_0}{\rho} = \frac{R^2}{r^2} \frac{dR}{dr} \tag{6.4}$$

where r is the Lagrangian coordinate.

The initial velocities were then calculated directly from the equation

$$u = \frac{\dot{Y}}{(\gamma + 1)^{1/3}} \frac{1 + \left(\frac{r}{Y}\right)^{3(\gamma-1)/\gamma}}{\left[1 + \gamma\left(\frac{r}{Y}\right)^{3(\gamma-1)/\gamma}\right]^{2/3}} \tag{6.5}$$

which follows from the small $\gamma - 1$ approximation. Here the correct shock velocity $\dot{Y}$ for the given shock pressure was used.

6.3 The Total Energy

The methods used to establish suitable initial conditions are in parts somewhat arbitrary. For this reason it is not surprising that the total energy corresponding to these conditions turned out to deviate appreciably from the assumed value of 10,000 tons of TNT. Unfortunately, the energy was recalculated from the initial conditions only after the IBM run had been completed. It was then found that the total energy was 13,500 tons TNT.

Since the initial shock pressure of 77.25 atm at the initial shock radius of 79.9 meters corresponds to an energy release of 10,000 tons, we have no remedy for the discrepancy. All that can be said is that the shock pressure vs distance curve corresponds to 10,000 tons up to 80 meter shock radius and to 13,500 tons for large radii. For intermediate radii it should slowly change between these values.

Actually the discrepancy is slightly less. A check of the total energy at a shock radius of 2000 meters gave only 13,100 tons. The "loss" of 400 tons is entirely due to errors of the IBM run and is of the order of magnitude to be expected from this source.

For most purposes the total energy in the IBM run should be assumed to be about 13,000 tons, except at small shock radii, where 10,000 tons is more appropriate.

6.4 The IBM Run

The hydrodynamical equations are

$$\rho_0 \frac{\partial^2 R}{\partial t^2} + \frac{R^2}{r^2} \frac{\partial p}{\partial r} = 0 \tag{6.6}$$

$$\frac{\rho_0}{\rho} = \frac{R^2}{r^2} \frac{dR}{dr} \tag{6.7}$$

In addition we have the equation of the adiabatics which were put in the form

$$\frac{p}{p_0} = g\left(\frac{\rho}{\rho_0}\right)^{1.5} + \eta \frac{\rho}{\rho_0} \tag{6.8}$$

where g and η are numerically known functions of the entropy.

The boundary conditions are that the velocity $\partial R/\partial t$ vanish at the center and that at the shock radius the Hugoniot conditions be satisfied. The latter determine also the entropy of any mass point as it passes through the shock front. The entropy is assumed to remain constant, so that essentially g and η are given functions of the Lagrange variable r.

The method employed first in solving the system of partial differential equations by means of the IBM machines was suitable as long as the shock pressure differed appreciably from 1 atm, but it became erratic as the overpressure became small. The method was therefore changed, so as to calculate changes in density and pressure rather than their absolute values. This change of procedure quickly suppressed the erratic behavior of the pressure.

The run was continued until the shock radius had reached a value of 6.270 meters. At that instant the overpressure in the shock was 0.0251 atm. The positive pulse was 290 meters long and the negative pulse 760 meters. Since the further propagation of the shock is influenced at these low overpressures only by the positive pulse, the approximations on which the semi-acoustic theory of Chapter 5 are based are well satisfied. They are (1) that the overpressure be small compared to 1 atm, and (2) that the length of the pressure pulse be small compared to the shock radius. Even the application of the semi-acoustic theory to the negative phase is not bad. Hence, the IBM run was discontinued and the semi-acoustic theory was used for the purpose of continuation.

6.5 Results

The shock pressure as a function of the distance of the shock front from the center of the explosion is shown in Fig. 6.1.

In this graph all data have been collected from the previous chapters, as well as from calculations which do not appear in this volume. From a shock radius of 10 to 80 meters the similarity solution has been used. The dotted lines show upper and lower limits for the effect of the bomb material on the propagation of the shock, as calculated for the Trinity test (sealed down to 10,000 tons of TNT). In this region the curve corresponds to an energy release of 10,000 tons.

For shock radii from 80 to 6300 meters, the shock pressures are obtained from the IBM run. Here the total energy is between 10,000 and 13,000 tons, the upper value being correct at sufficiently large distances. The time of arrival of the shock is indicated at various points. T = 0 is the start of the IBM run which was 0.012 sec after the explosion.

Beyond a radius of 6300 meters up to 67,000 meters, the semi-acoustic theory of Chapter 5 has been used.

A number of curves showing the pressure at a fixed distance as function of time are shown in Figs. 6.2 to 6.4. Graphs of the pressure vs distance at a fixed time are shown in Figs. 6.5 to 6.13.

The duration of the positive phase of the pulse as function of the shock pressure is given in Fig. 6.14.

Finally, there are shown in Fig. 6.15 the positive impulse I+ and the fraction of the total energy which is left in the blast as functions of the shock pressure divided by the normal pressure. The latter is independent of the energy release. The positive impulse has been scaled to an energy release of 40,000 tons in free air (or 20,000 tons on the ground) for the purpose of comparison with observations at Trinity.

6.6 Comparison with TNT Explosion. Efficiency of Nuclear Explosion

One purpose of the IBM run was to find the efficiency of a nuclear explosion compared to an explosion from an equivalent charge of TNT. In the nuclear explosion a greater amount of energy is used for the purpose of heating the air near the center of the explosion to high temperatures. A large fraction of this energy is useless for the propagation of the shock.

Since no comparable IBM run exists for a TNT explosion, we compared the results for the nuclear explosion with experimental data. For this purpose, the experimental curve prepared by Hirschfelder, Littler and Sheard[4] was used. It is based on experimental data for charges fired on the ground, and for shock pressures in the range from 15 to 2 pounds per square inch. The charges varied from 67 to 550 pounds. The curve is given by the expression

$$\Delta p = \frac{38.5}{x} + \frac{85}{x^2} + \frac{5760}{x^3} \qquad (6.9)$$

$$x = Y/w^{1/3} \qquad (6.10)$$

Here Y is the shock radius in feet; w the weight of the charge in pounds; and Δp the overpressure in psi.

4. Hirschfelder, Littler and Sheard, Estimated Blast Pressures from TNT charges of 2 to 10,000 tons, Los Alamos Scientific Laboratory Report LA-316, June 25, 1945 (classified).

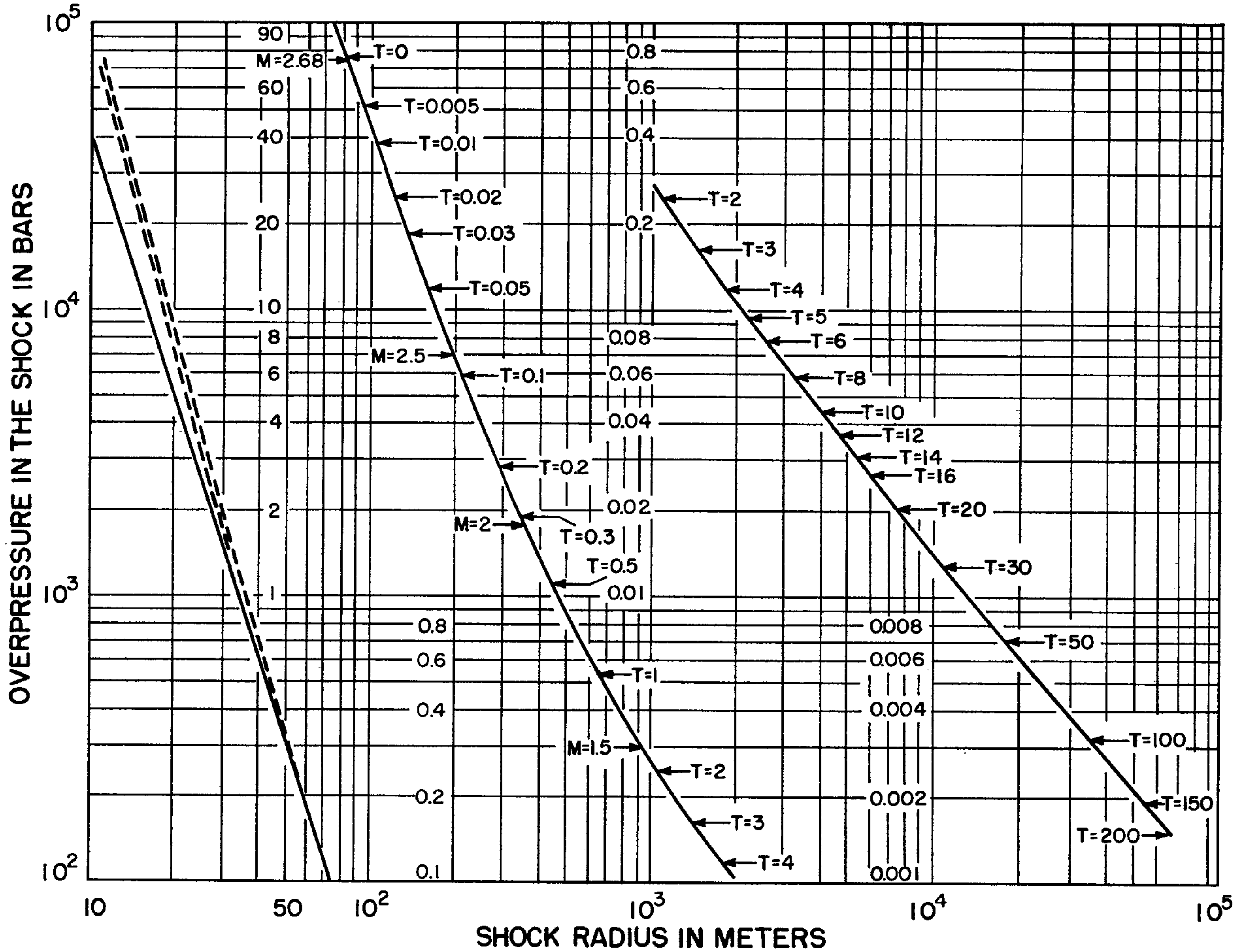

Fig. 6.1 Shock pressure vs distance for nuclear explosion. Time is given in seconds; T = 0 is start of IBM run, 0.012 sec after explosion.